Sustained Activation of the Unfolded Protein Response Induces Cell Death in Fuchs' Endothelial Corneal Dystrophy

Naoki Okumura,[1] Miu Kitahara,[1] Hirokazu Okuda,[1] Keisuke Hashimoto,[1] Emi Ueda,[1] Makiko Nakahara,[1] Shigeru Kinoshita,[2] Robert D. Young,[3] Andrew J. Quantock,[3] Theofilos Tourtas,[4] Ursula Schlötzer-Schrehardt,[4] Friedrich Kruse,[4] and Noriko Koizumi[1]

[1]Department of Biomedical Engineering, Faculty of Life and Medical Sciences, Doshisha University, Kyotanabe, Japan
[2]Department of Frontier Medical Science and Technology for Ophthalmology, Kyoto Prefectural University of Medicine, Kyoto, Japan
[3]Structural Biophysics Group, School of Optometry and Vision Sciences, Cardiff University, Cardiff, United Kingdom
[4]Department of Ophthalmology, University of Erlangen-Nürnberg, Erlangen, Germany

Correspondence: Noriko Koizumi, Department of Biomedical Engineering, Faculty of Life and Medical Sciences, Doshisha University, Kyotanabe 610-0321, Japan; nkoizumi@mail.doshisha.ac.jp.

Submitted: October 31, 2016
Accepted: May 21, 2017

Citation: Okumura N, Kitahara M, Okuda H, et al. Sustained activation of the unfolded protein response induces cell death in Fuchs' endothelial corneal dystrophy. *Invest Ophthalmol Vis Sci*. 2017;58:3697–3707. DOI: 10.1167/iovs.16-21023

Purpose. The unfolded protein response (UPR) is believed to play a role in the pathogenesis of Fuchs' endothelial corneal dystrophy (FECD). The purpose of this study was to investigate whether unfolded proteins accumulate in the corneal endothelium in FECD and if they are involved in triggering cell death.

Methods. Descemet's membranes with corneal endothelial cells (CECs) were obtained during keratoplasty, and expression of aggresomes, type 1 collagen, fibronectin, and agrin was evaluated. Endoplasmic reticulum (ER) stress of immortalized human CECs from non-FECD subjects and from FECD patients (iHCEC and iFECD, respectively) were evaluated. The effect of MG132-mediated aggresome formation on the UPR and intrinsic pathway and the effect of mitochondrial damage on UPR were also examined. The effect of CHOP knockdown on the ER stress–mediated intrinsic pathway was also evaluated.

Results. Aggresome formation was higher in iFECD than in iHCEC and was colocalized with type 1 collagen, fibronectin, and agrin. GRP78, phosphorylated IRE1, PERK, and CHOP showed higher activation in iFECD than in iHCEC. MG132-mediated aggresome formation upregulated ER stress sensors, the mitochondrial membrane potential drop, cytochrome c release to the cytoplasm, and activation of caspase-9 and -3. By contrast, staurosporine-mediated mitochondrial damage did not induce ER stress. Knockdown of CHOP attenuated the ER stress-induced cleavage of caspase-9, which is caused by intrinsic pathway activation.

Conclusions. Excessive synthesis of extracellular matrix proteins induced unfolded protein accumulation in FECD. Prolonged ER stress–mediated cell death, occurring via the intrinsic apoptotic signaling pathway, therefore might be associated with the pathogenesis of FECD.

Keywords: Fuchs' endothelial corneal dystrophy, unfolded protein response, apoptosis, corneal endothelial cells

Fuchs' endothelial corneal dystrophy (FECD) is a bilateral and slowly progressive primary disease of the corneal endothelium. It is clinically categorized into three stages: (1) the presence of guttae without corneal edema, (2) the presence of guttae with stromal or epithelial edema, and (3) corneal scarring or neovascularization caused by long-standing corneal edema. The prevalence of FECD in the United States has been estimated to be as high as 4% of the population older than 40 years.[1] In agreement with this high prevalence, visual disturbance due to FECD is the leading cause of corneal transplantation. Recent data show that 15,707 (21.7%) of the 72,465 corneas provided by eye banks in the United States were used to treat FECD.[2]

Histological analysis has suggested that the corneal endothelial cell (CEC) loss occurring in FECD is due to apoptosis,[3–5] but the pathophysiologic cause of this apoptosis has not been identified. In 2010, Engler and colleagues[6] showed morphological alterations of the endoplasmic reticulum (ER), and upregulation of markers of the unfolded protein response (UPR), such as glucose-regulated protein (GRP78), α subunit of eukaryotic initiation factor 2 (eIF2α), and CCAAT-enhancer-binding protein homologous protein (CHOP) in the corneal endothelium of FECD patients. Hence, they postulated that the UPR plays an important role in the pathogenesis of FECD.[6] The same research group subsequently showed the involvement of the UPR in the CEC loss in an alpha 2 collagen VIII transgenic knock-in mouse, an animal model of early-onset FECD.[7]

The ER is the membranous tubular network that participates in cellular protein biosynthesis, lipid biosynthesis, and calcium homeostasis. Newly synthesized proteins mature and undergo proper folding in the ER.[8] A wide range of stresses, including increased secretory protein production, glucose deprivation, and hypoxia, induces the accumulation of unfolded or misfolded proteins in the ER lumen.[9,10] The conditions within

the ER are monitored by the UPR signaling pathway, and activation of the UPR restores protein folding homeostasis by reducing protein translation, increasing ER chaperone expression, and degrading misfolded proteins.[9–11] However, prolonged ER stress impairs protein homeostasis, which then triggers the UPR to induce apoptosis.[9,10,12] Consequently, targeting the UPR has emerged as a promising therapeutic modality for the treatment of diseases related to accumulation of unfolded or misfolded proteins in the ER.[13–15]

Our aim in the present study was to investigate the potential involvement of the UPR in FECD as a possible contributor to the underlying pathophysiological mechanism. Here, we have investigated the accumulation of unfolded or misfolded proteins in the corneal endothelium with the goal of detecting any functional links between the UPR and apoptosis of CECs in FECD.

Methods

Ethics Statement

The human tissue used in this study was handled under the guidelines based on the ethical principles of the Declaration of Helsinki. This study was performed according to a protocol approved by the ethical review committee of the Friedrich-Alexander University Erlangen-Nürnberg. Informed consent was acquired from the patients with FECD, and stripped Descemet's membranes with CECs were obtained during Descemet's membrane endothelial keratoplasty (DMEK). Normal human donor corneas were obtained from SightLife (Seattle, WA, USA; http://www.sightlife.org/). Informed written consent was obtained from the next of kin of all deceased donors with regard to eye donation for research. All tissue specimens were recovered under the tenets of the Uniform Anatomical Gift Act of the particular state in which the donor consent was obtained and the tissue recovered.

Cell Culture

The immortalized CECs from three patients with FECD were used as a cell model, and the immortalized CECs from three donor corneas were used as control (hereafter iFECD and iHCEC, respectively). Both iFECD and iHCEC were passaged from 30 to 40 times before use in these experiments. Descemet's membranes, including the CECs, were stripped from the corneas of patients with FECD during DMEK and used for cell cultivation. Three patients with FECD and the three donors of the non-FECD subject were older than 50 years.

The iFECD and iHCEC were cultured according to published protocols.[16,17] Briefly, the FECD-derived CECs and the control CEC were cultured for 14–21 days and then immortalized using SV40 and hTERT to produce iFECD and iHCEC cell lines, respectively. The coding sequences of the SV40 large T antigen and hTERT genes were amplified by PCR and were TA-cloned into a commercial lentiviral vector. The lentiviral vectors were transfected to human embryonic kidney 293T cells (RCB2202; Riken Bioresource Center, Ibaraki, Japan) along with three helper plasmids (pLP1, pLP2, and pLP/VSVG) using a transfection reagent. After 48 hours of transfection, the supernatant of the culture medium was harvested. For lentiviral transduction, the virus-containing supernatants of both genes were added to the cultures of HCECs in the presence of 5 μg/mL of polybrene. The immortalized cells were cultured in Dulbecco's modified Eagle's medium (DMEM; Life Technologies Corp., Carlsbad, CA, USA) containing 10% fetal bovine serum and 1% penicillin and streptomycin (Life Technologies Corp.). Once the cells were 80% confluent, the cells were trypsinized with 0.05% Trypsin-EDTA and passaged.

The iHCEC were cultured with DMEM supplemented with thapsigargin (10 μM; Wako Pure Chemical Industries, Ltd., Tokyo, Japan), and tunicamycin (30 μg/mL; Wako Pure Chemical Industries, Ltd.) to induce ER stress. The iHCEC were cultured with DMEM supplemented with staurosporine (0.5 μM; Sigma-Aldrich Corp., St. Louis, MO, USA) to induce apoptosis via the mitochondrial pathway. Unfolded protein aggregation was induced with MG132 (0.5 μM; Sigma-Aldrich Corp.).

Transmission Electron Microscopy (TEM)

Ultrastructural analysis of corneal specimens was performed on full-thickness corneas obtained during penetrating keratoplasty from patients with FECD ($n = 5$, mean age 63.3 ± 7.5 years) to assess whether the morphology of the ER and mitochondria was altered. Donor corneas from the non-FECD subjects were evaluated as a control. The central corneal endothelium was evaluated in FECD and in non-FECD subjects. Tissue specimens were fixed in 2.5% glutaraldehyde in 0.1 M phosphate buffer, postfixed in 2% buffered osmium tetroxide, dehydrated in graded alcohol concentrations, and embedded in epoxy resin, according to standard protocols. For analysis of cultured CECs, 1×10^5 cells were seeded onto Corning Transwell polyester membrane cell culture inserts (Corning, Inc., Corning, NY, USA) and grown until confluent. The entire Transwell inserts were fixed with 2.5% glutaraldehyde, 2% paraformaldehyde in 0.1 M Sorensen phosphate buffer. The Transwell membrane samples were washed in 0.1 M Sorensen phosphate buffer, processed through 0.5% uranyl acetate for en bloc staining, and subsequently dehydrated using an ascending ethanol series. The specimens were transferred to propylene oxide and then infiltrated and embedded in Araldite CY212 resin. Ultrathin sections were collected on uncoated G300 copper grids and stained with 1% aqueous phosphotungstic acid and uranyl acetate. Sections were examined with a transmission electron microscope (JEOL 1010; JEOL, Tokyo, Japan) equipped with a charge-coupled device camera (Orius SC1000; Gatan, Pleasanton, CA, USA).

Immunocytochemistry and Aggresome Staining

Descemet's membranes with CECs, obtained from 21 FECD patients during DMEK or from donor corneas from 20 non-FECD control subjects, and cultured CECs were fixed with 4% paraformaldehyde at room temperature for 10 minutes on glass slides. Excess paraformaldehyde was removed by washing with Dulbecco's PBS, and the samples were permeabilized with 0.5% Triton X-100 (Nacalai Tesque, Kyoto, Japan), and then incubated with 1% BSA to block nonspecific binding. The samples were incubated with primary antibodies against GRP78 (1:200; Santa Cruz Biotechnology, Santa Cruz, CA, USA), collagen I (1:200; Sigma-Aldrich Corp.), fibronectin (1:200; BD Biosciences, San Jose, CA, USA), agrin (1:200; Santa Cruz Biotechnology), and CHOP (1:200; Santa Cruz Biotechnology). Alexa Fluor 488-conjugated goat anti-mouse (Thermo Fisher Scientific, Waltham, MA, USA) antibodies were used as secondary antibodies at a 1:1000 dilution. For aggresome staining, samples were incubated with aggresome reagent (1:2000; Enzo Life Science Inc., Farmingdale, NY, USA) for 60 minutes. Nuclei were stained with 4′,6-diamidino-2-phenylindole (DAPI; Vector Laboratories, Burlingame, CA, USA). The slides were examined with a fluorescence microscope (DM 2500; Leica Microsystems, Wetzlar, Germany).

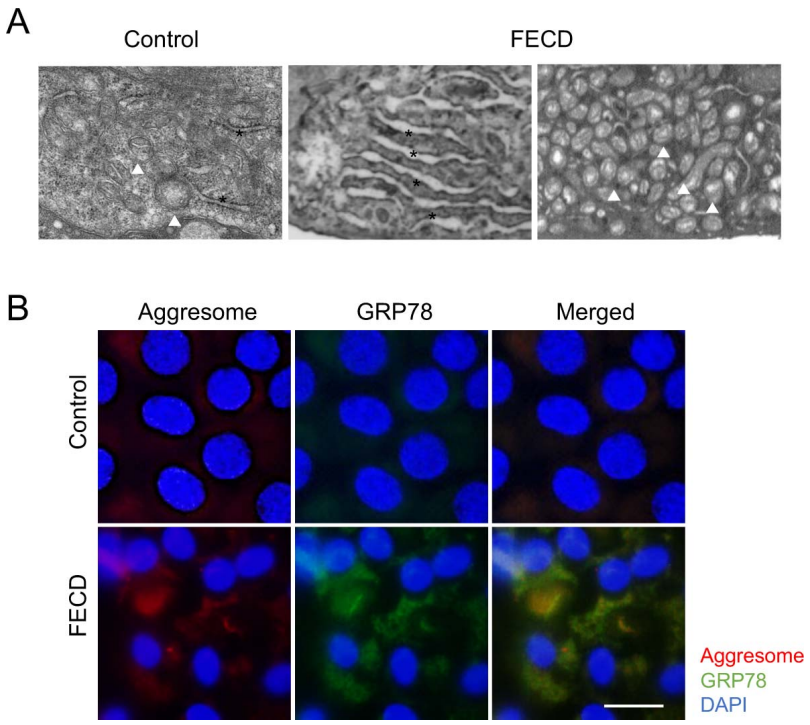

Figure 1. Accumulation of aggresomes in the corneal endothelium of FECD patients. (**A**) Corneal endothelium was evaluated by TEM. Representative TEM of non-FECD subject is shown as a control (*left*). Representative TEM of patients with FECD shows that ER is evident with morphological change with dilation in the corneal endothelium (*middle*). The morphology of the mitochondria is also altered and some mitochondria are dilated (*right*). *Asterisks* indicate ER, and *arrowheads* indicate mitochondria. (**B**) Descemet's membranes with corneal endothelium were obtained during DMEK, and stained for aggresomes and GRP78. Donor corneas were used as controls. A representative aggresome staining image shows diffuse staining and aggregations in the FECD but not in the control sample. Expression of GRP78 was higher in FECD samples and widely colocalized with aggresomes. Experimental findings were confirmed in at least 10 independent samples. Nuclei were stained with DAPI. *Scale bar*: 20 μm.

Quantitative Real-Time PCR

Gene expression levels were analyzed using TaqMan real-time PCR. Total RNA was extracted from the corneal endothelium from 10 patients with FECD and 10 donor corneas using the miRNeasy Mini Kit (Qiagen, Hilden, Germany). Then, cDNA was synthesized by SuperScript VILO MasterMix (Thermo Fisher Scientific). For quantification, standard curves using serial dilutions (10^2–10^7 copies) of plasmid-cloned amplicons were run in parallel. For normalization of gene expression levels, ratios relative to glyceraldehyde 3-phosphate dehydrogenase (GAPDH) were calculated.

The TaqMan primers used were for *COL1A1*, Hs00164004_ml; *FN1*, Hs00365052_ml; *AGRN*, Hs00394748_ml; and TaqMan predevelopment human GAPDH (Applied Biosystems, Foster City, CA, USA). The PCR was performed using the StepOne (Applied Biosystems) real-time PCR system. GAPDH was used as an internal standard.

Mitochondrial Membrane Potential

The iFECD and iHCEC were stained with 5,5′,6,6′-tetrachloro-1,1′,3,3′-tetraethylbenzimidazolylcarbocyanine iodide (JC-1) and the mitochondrial membrane potential was evaluated by fluorescence microscopy and flow cytometry, according to the manufacturer's protocol. Briefly, iFECD and iHCEC were cultured in medium supplemented with carbonyl cyanide-m-chlorophenylhydrazone (CCCP) (50 μM; Abcam, Cambridge, UK) for 9 hours as positive controls. For fluorescence microscopy analysis, the cells were incubated with MitoScreen (10 μM; BD Biosciences) for 15 minutes and fixed with 4% formaldehyde for 10 minutes, washed with PBS, and nuclei were stained with DAPI. The slides were examined with a fluorescence microscope (DMI 4000B; Leica Microsystems, Wetzlar, Germany). For flow cytometry, cells were washed twice with PBS and incubated with Accumax (Innovative Cell Technologies, San Diego, CA, USA) for 10 minutes at 37°C. The cells were recovered in Assay buffer supplemented with MitoScreen (10 μM; BD Biosciences), incubated for 15 minutes at 4°C, washed three times with PBS, and then resuspended in FACS buffer and analyzed by flow cytometry using CellQuest Pro software (BD Biosciences).

Immunoblotting

The cultured CECs were washed with ice-cold PBS and lysed with ice-cold RIPA buffer containing phosphatase inhibitor cocktail 2 (Sigma-Aldrich Corp.) and protease inhibitor cocktail (Roche Applied Science, Penzberg, Germany). Following centrifugation, the supernatant containing the total proteins was fractionated by SDS-PAGE. The separated proteins were transferred to polyvinylidene difluoride membranes, blocked with 3% nonfat dry milk, and incubated overnight at 4°C with the following primary antibodies: pancreatic ER kinase (PERK) (1:1000; Cell Signaling Technology, Inc., Danvers, MA, USA), phosphorylated PERK (1:1000; Cell Signaling Technology, Inc.), activating transcription factor 6α (ATF6α) (1:1000; Bio Academia, Inc., Osaka, Japan), inositol-requiring transmembrane kinase/endonuclease 1α (IRE1α) (1:1000; Cell Signaling Technology), phosphorylated IRE1α (1:1000; Novus Biologicals, Littleton, CO, USA), spliced active form of X-box binding protein 1 (XBP1s) (1:1000; BioLegend, San Diego, CA, USA), bcl2 (1:1000; Cell Signaling Technology), caspase-9 (1:1000;

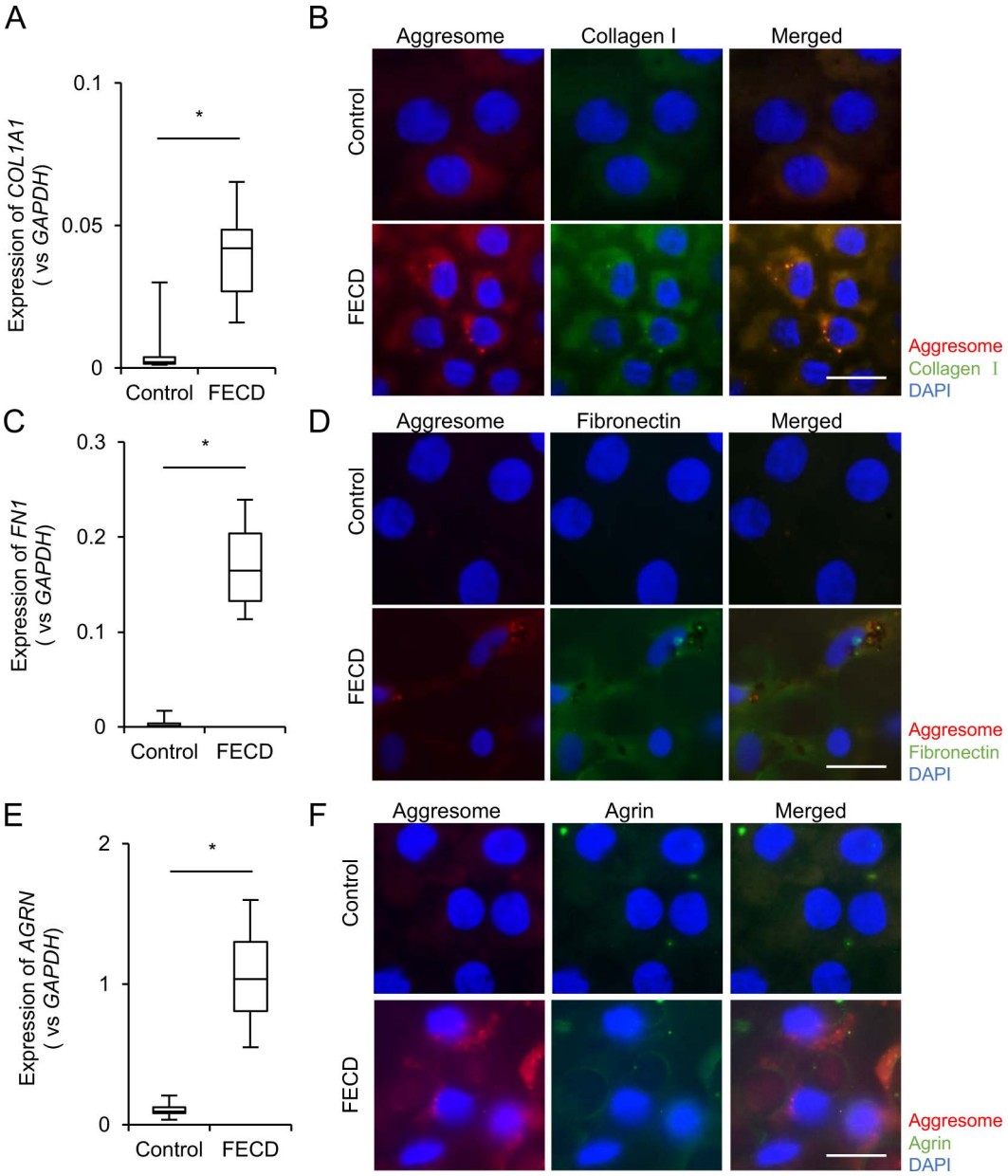

Figure 2. Involvement of ECM proteins and proteoglycan in the formation of aggresomes. (**A**, **C**, **E**) Total RNA was extracted from the corneal endothelium of the 30 patients with FECD and 30 donor corneas. Expression of type 1 collagen, fibronectin, and agrin in the corneal endothelium was determined by quantitative PCR. The mRNA expression of type 1 collagen, fibronectin, and agrin was significantly higher in FECD than in the control. $^*P < 0.01$. (**B**, **D**, **F**) Immunofluorescence staining showed that type 1 collagen, fibronectin, and agrin were more highly expressed in FECD than in control samples. Not all, but a certain amount of type 1 collagen, fibronectin, and agrin, was colocalized with aggresomes. Experimental findings were confirmed in at least 10 independent samples. Nuclei were stained with DAPI. *Scale bar*: 20 μm.

Cell Signaling Technology), caspase-3 (1:1000; Cell Signaling Technology), poly (ADP-ribose) polymerase (PARP) (1:2000; Cell Signaling Technology), CHOP (1:1000; Cell Signaling Technology), cytochrome c (BD Biosciences), voltage-dependent anion channel (VDAC; Cell Signaling Technology), and GAPDH (1:3000; Medical and Biological Laboratories Co., Ltd., Aichi, Japan). The blots were probed with horseradish peroxidase–conjugated secondary antibodies (1:5000; GE Healthcare, Piscataway, NJ, USA), developed with luminal for enhanced chemiluminescence using the ECL Advanced Western Blotting Detection Kit (Nacalai Tesque), and documented with an LAS4000S (Fuji Film, Tokyo, Japan) cooled charge-coupled-device camera gel documentation system. The relative density of immunoblot bands was determined using ImageJ software (http://imagej.nih.gov/ij/; provided in the public domain by the National Institutes of Health, Bethesda, MD, USA). Molecular weight markers (Bio-Rad, Hercules, CA, USA) were run alongside all samples.

For the assessment of release of cytochrome c from mitochondria to the cytoplasm, 5×10^5 iHCEC were seeded on a 10-cm culture dish, cultured for 24 hours, and then further incubated with fresh DMEM supplemented with thapsigargin (10 μM) tunicamycin (30 μg/mL), or MG132 for 24 hours. Cytoplasmic protein was isolated from mitochondrial protein by Mitochondria Isolation Kit (Thermo Fisher Scientific) according to manufacturer's protocol. Briefly, harvested cells were centrifuged at 800*g*, Mitochondria Isolation Reagent A was added to the tube, and the sample was stored on ice for

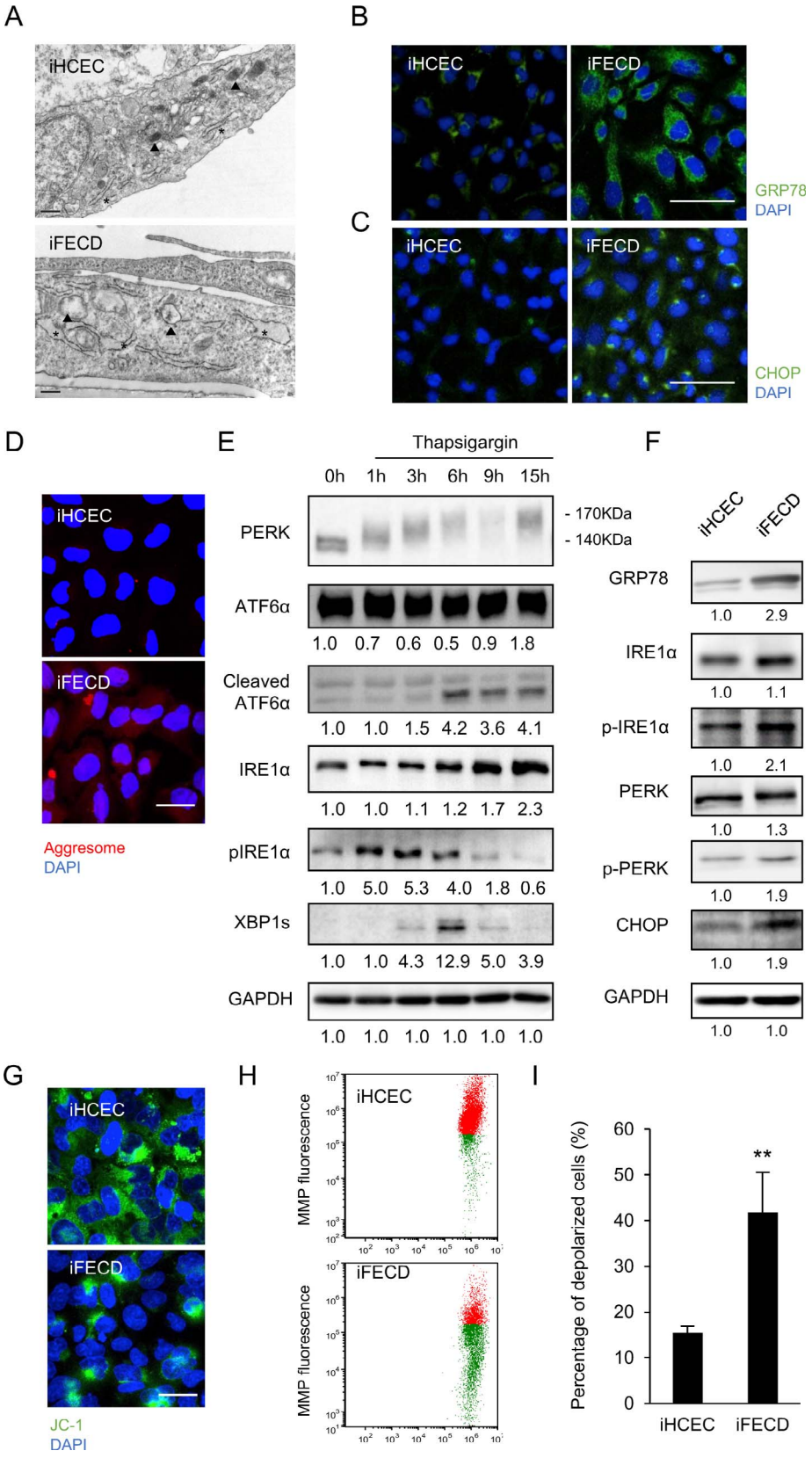

Figure 3. Accumulation of aggresomes and mitochondrial membrane depolarization in the FECD cell model. (**A**) The immortalized CECs from FECD patients (hereafter iFECD) were used as a cell model, and the immortalized CECs from donor corneas (hereafter, iHCEC) were used as controls. The iFECD and iHCEC cultured on Corning Transwell polyester membrane cell culture inserts were analyzed by TEM. ER was dilated, and mitochondria were dilated associated with altered inner structure morphology in iFECD, but not in iHCEC. *Asterisks* indicate ER, and *arrowheads* indicate mitochondria. (**B**, **C**) Immunofluorescence staining showed that strong expression of GRP78 and CHOP was observed in iFECD when compared with iHCEC. Nuclei were stained with DAPI. Experiments were performed on three independent samples. *Scale bar*: 40 μm. (**D**) iFECD

and iHCEC were cultured on culture plates and examined for formation of aggresomes. A high level of aggresome formation was observed in iFECD, but not in iHCEC. Nuclei were stained with DAPI. Experiments were performed on three independent samples. *Scale bar*: 50 μm. (**E**) The iHCEC established from donor corneas were cultured and stimulated with thapsigargin to induce ER stress. Western blotting showed that thapsigargin treatment induced the phosphorylation of PERK, cleavage of ATF6, and phosphorylation of IRE1 associated with XBP1 cleavage. The relative density of immunoblot bands in triplicate experiments was determined using ImageJ software. Relative fold differences were compared with the values at 0 hour. (**F**) Activation of ER stress–related proteins in iHCEC and iFECD was evaluated by Western blotting. Expression of GRP78, phosphorylated IRE1α and PERK, and CHOP was higher in iFECD than in iHCEC. The relative density of immunoblot bands was determined using ImageJ software. Experiments were performed using two iHCEC established from two independent non-FECD donor corneas and two iFECD established from two independent FECD donors. (**G**) JC-1 staining showed greater depolarization of the mitochondrial membrane potential in iFECD than in iHCEC. Nuclei were stained with DAPI. Experiments were performed on three independent samples. *Scale bar*: 50 μm. (**H**) Flow cytometry also showed greater depolarization of the mitochondrial membrane potential in iFECD than in iHCEC. *Red dots* indicate cells with normal mitochondrial membrane potential and *green dots* indicate cells with depolarized mitochondrial membrane potential. (**I**) Flow cytometry showed that 15.5% of iHCEC exhibited depolarization of mitochondrial membrane potential, but 41.7% of iFECD exhibited this depolarization ($n = 3$). Experiments were performed in triplicate. $^*P < 0.01$.

2 minutes. Then, Mitochondria Isolation Reagent B and Mitochondria Isolation Reagent C were added, and the tube was centrifuged at 700*g*. The supernatant was recovered, and centrifuged again. This final supernatant was recovered as cytoplasmic protein, and was used for Western blotting.

Knockdown of Genes by Small Interfering RNA (siRNA)

The iHCEC were seeded into a 24-well plate and cultured until they reached 50% to 70% confluence. The iHCEC were then incubated with RNAi duplex (DDIT3) and Lipofectamine RNAiMAX (Thermo Fisher Scientific), according to the manufacturer's protocol. Random RNAi low GC was used as a control and RT-PCR was performed to assess the knockdown of DDIT3.

Statistical Analysis

The statistical significance (*P* value) of differences between mean values of the two-sample comparison was determined with the Student's *t*-test. The comparison of multiple sample sets was analyzed using Dunnett's multiple-comparison test. The data represent the mean ± SEM.

Results

Accumulation of Unfolded Proteins in the Corneal Endothelium of Patients With FECD

Examination of the corneal endothelium of corneas obtained from FECD patients by TEM frequently showed ultrastructural alterations of the ER, mainly prominent and dilated ER cisternae (Fig. 1A; middle) in comparison with the non-FECD subject (Fig. 1A; left). Morphological alterations observed in the mitochondria included focal loss of cristae and distended shape (Fig. 1A; right). These morphological alterations in ER and mitochondria motivated us to determine the involvement of ER and mitochondria in the pathophysiology of FECD. We evaluated the extent of the accumulation of unfolded proteins in the FECD corneal endothelium. The CEC-Descemet's membrane whole mounts demonstrated higher levels of diffuse aggresome staining and perinuclear aggregations in the FECD specimens than in the control specimens (Fig. 1B). This increased expression of aggresomes in FECD samples was confirmed in all 21 individual Descemet's membranes. Double labeling of aggresomes and GRP78, which mediates the protein folding processes,[18] showed higher expression of GRP78 in FECD samples and a wide colocalization with aggresomes, suggesting the presence of increased amounts of unfolded or misfolded protein and subsequent UPR in the endothelial cells from patients with FECD (Fig. 1B).

We next evaluated the involvement of extracellular matrix (ECM) components, as these are produced by corneal endothelium in FECD and accumulate in guttae or thickened Descemet's membrane in the form of aggresomes. Similar to previous reports,[19,20] quantitative PCR showed that mRNA expression of type I collagen, fibronectin, and agrin was higher in patients with FECD than in controls (Figs. 2A, 2C, 2E; respectively). Correspondingly, immunofluorescence staining showed that protein expression of type I collagen, fibronectin, and agrin was higher in endothelial cells from FECD specimens than from control specimens. Interestingly, type I collagen, fibronectin, and agrin were found to partially colocalize with aggresomes, implying that excessive production of ECM components contributes to aggresome formation in the corneal endothelium in FECD (Figs. 2B, 2D, 2F).

Evaluation of the Involvement of the UPR in an FECD Cell Model

We previously established a cell model of FECD (iFECD) by culturing and immortalizing the CEC derived from FECD patients and control CEC derived from donor corneas (iHCEC).[16] Here, we used this model to evaluate the involvement of the UPR and its effects on mitochondria. Similar to the findings for surgical specimens, TEM observations revealed ultrastructural alterations, such as dilated ER cisternae and swollen mitochondria with partial loss of cristae, in iFECD but not in iHCEC (Fig. 3A). Asterisks indicate the ER, and arrowheads indicate mitochondria. Immunofluorescence microscopy showed higher expression levels of GRP78 and CHOP (an apoptosis inducer that is activated by ER stress) in iFECD than in iHCEC (Figs. 3B, 3C, respectively). Aggresome staining showed higher amounts of unfolded protein associated with aggregation in iFECD than in iHCEC (Fig. 3D).

These cells were then characterized for expression of three proximal sensors of the UPR: PERK, IRE1α, and ATF6α.[21] Treatment of iHCEC with thapsigargin, which acts as an ER stress inducer by specifically inhibiting the ER Ca^{2+}-ATPase,[22] increased the phosphorylation of PERK, the cleavage of ATF6, and the phosphorylation of IRE1. IRE1α is a protein kinase that initiates unconventional splicing of Xbp-1 mRNA to produce an active transcription factor,[21] and Western blotting showed that XBP1 expression was induced by thapsigargin stimulation (Fig. 3E; Supplementary Fig. S1). These results provide evidence that the UPR sensors, PERK, IRE1a, and ATF6a, are conserved in corneal endothelium to sense the ER stress. Consistent with the immunofluorescence images shown in Figures 3B and 3C, Western blotting showed that expression of GRP78 and CHOP was higher in iFECD than in iHCEC. We also evaluated the activation of IRE1α and PERK, which induces apoptosis due to ER stress, and showed that phosphorylation of PERK and of IRE1α was higher in iFECD than in iHCEC (Fig. 3F). Consistent

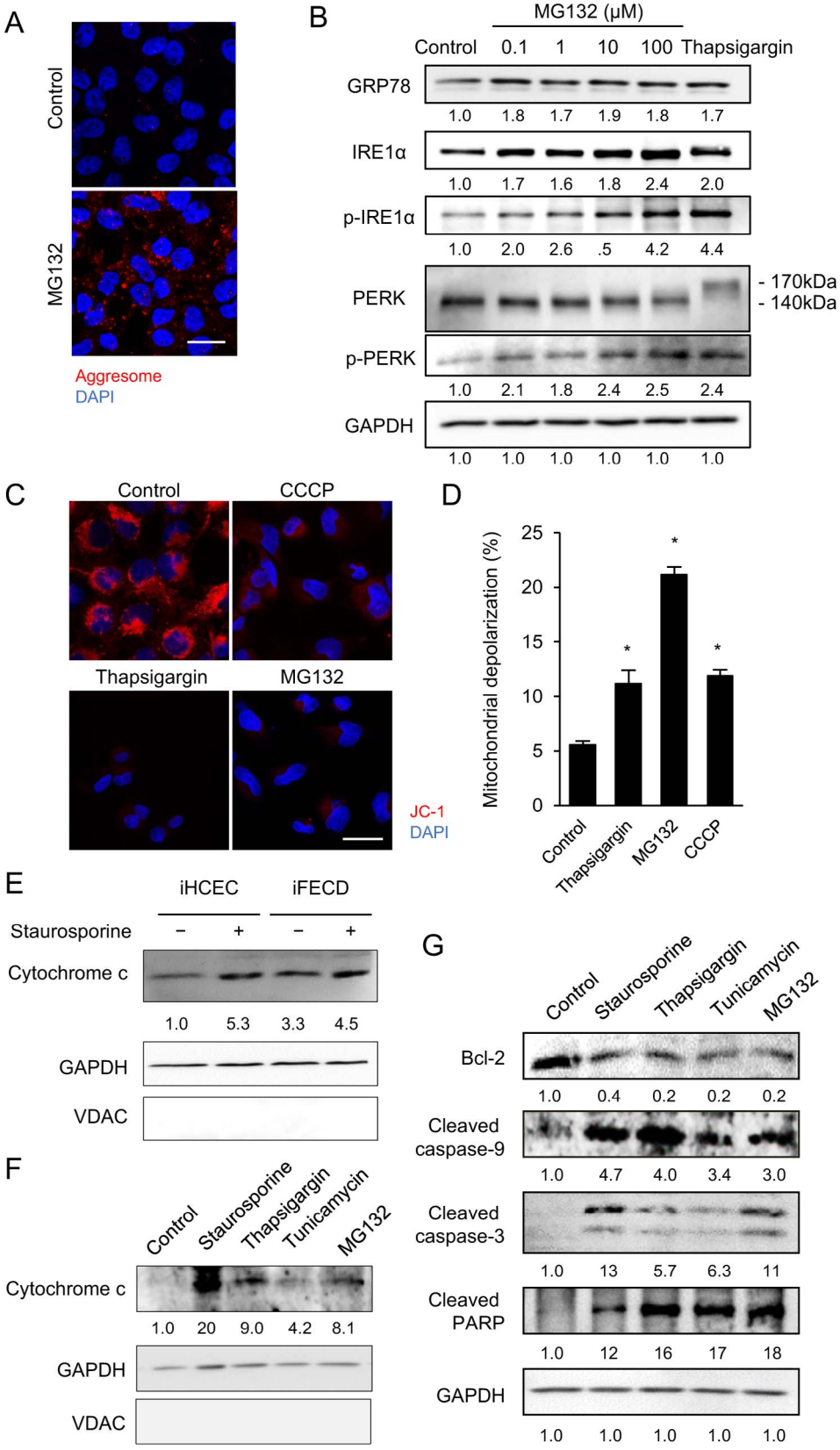

Figure 4. Involvement of aggresomes in mitochondrial pathway activation. (**A**) iHCEC were treated with 10 μM MG132 (a proteasome inhibitor), which reduces the degradation of ubiquitin-conjugated proteins to induce aggresome formation. *Scale bar*: 50 μm. (**B**) iHCEC were treated with MG132 or 10 μM thapsigargin as positive controls for 24 hours. Western blotting showed that MG132 treatment upregulated expression of GRP78, phosphorylation of IRE1α, and expression of PERK. The relative density of immunoblot bands in duplicate experiments was determined using ImageJ software. Relative fold differences were compared with the values of the control. (**C**) iHCEC were stimulated with CCCP, thapsigargin, and MG132, followed by evaluation of the mitochondrial membrane potential by JC-1 staining. Thapsigargin-mediated ER stress decreased mitochondrial

membrane potential, and MG132-mediated aggresome formation also decreased mitochondrial membrane potential. CCCP, a chemical inhibitor of oxidative phosphorylation, was used as a positive control for mitochondrial membrane potential depolarization. Experiments were performed in triplicate. Nuclei were stained with DAPI. *Scale bar*: 50 μm. (**D**) iHCEC were stimulated with CCCP, thapsigargin, and MG132, incubated in JC-1 staining reagent, and then evaluated for mitochondrial membrane potential by flow cytometry. Thapsigargin increased the depolarization of iHCEC mitochondria to 11.2% and MG132 increased this to 21.2%, whereas untreated control iHCEC depolarized at 5.6% ($n = 3$). Experiments were performed in triplicate. $^{*}P < 0.01$. (**E**) Release of cytochrome c from the mitochondria to the cytoplasm in iHCEC and iFECD was evaluated by Western blotting. Staurosporine was used as a positive control. Release of cytochrome c from the mitochondria to the cytoplasm was higher in iFECD than in iHCEC. The relative density of immunoblot bands was determined using ImageJ software. Experiments were performed by using two iHCEC established from two independent non-FECD donor corneas and two iFECD established from two independent FECD donors. (**F**) iHCEC were treated with staurosporine, thapsigargin, tunicamycin, and MG132. Staurosporine was used as a positive control, and it induced the release of cytochrome c from the mitochondria to the cytoplasm. Staurosporine, thapsigargin or tunicamycin caused ER stress and induced the release of cytochrome c. MG132-mediated aggresome formation also induced cytochrome c release. GAPDH was used as a cytoplasmic marker, and VDAC was used as a mitochondrial marker. The relative density of immunoblot bands in duplicate experiments was determined using ImageJ software. Relative fold differences were compared with the values of the control. (**G**) Western blotting showed that MG132 suppressed the expression of Bcl-2 and the cleavage of caspase-9, caspase-3, and PARP, as observed following thapsigargin- or tunicamycin-mediated ER stress. The relative density of immunoblot bands in triplicate experiments was determined using ImageJ software. Relative fold differences were compared with the values of control. Experiments were performed in triplicate.

with the morphological alterations of mitochondria observed with TEM, JC-1 staining showed greater depolarization of the mitochondrial membrane potential in iFECD than in iHCEC (Fig. 3G). Flow cytometry also showed significant greater depolarization of the mitochondrial membrane potential in iFECD than in iHCEC (Figs. 3H, 3I), suggesting that mitochondrial function is impaired in FECD.

Effect of Aggresome Formation on the UPR and Mitochondrial Function

We evaluated whether aggresome formation induces the UPR in CECs by treating iHCEC with the proteasome inhibitor MG132 in a similar manner to iFECD. Unfolded protein is degraded by the ubiquitin-proteasome system or folded properly by chaperone proteins, so even healthy cells will contain some amount of improperly folded protein. The MG132 treatment reduced the degradation of ubiquitin-conjugated proteins and induced aggresome formation in the iHCEC (Fig. 4A). MG132 treatment also upregulated the expression of GRP78 and the phosphorylation of IRE1α and PERK, indicating that MG132-mediated aggresome deposition induce ER stress (Fig. 4B). JC-1 staining showed that both thapsigargin-induced ER stress and MG132-mediated aggresome formation decreased the mitochondrial membrane potential. CCCP, a chemical inhibitor of oxidative phosphorylation, was used as a positive control (Figs. 4C, 4D). Cytochrome c is a component of the electron transport chain in mitochondria and is released from mitochondria into the cytoplasm during the initiation of apoptosis. Western blotting showed that the release of cytochrome c to the cytoplasm was higher in iFECD than in iHCEC (Fig. 4E). As was observed in iFECD, MG132 induced the release of cytochrome c to the cytoplasm in a similar manner to that observed with thapsigargin and tunicamycin, which both induce ER stress (Fig. 4F). Staurosporine was used as positive control (Fig. 4F). MG132 treatment suppressed the expression of Bcl-2, an integral outer mitochondrial membrane protein that blocks apoptotic cell death, and induced the cleavage of caspase-9, a proapoptotic protein activated by cytochrome c. In addition, MG132 treatment activated the execution caspase, caspase-3, as well as the downstream apoptosis-inducing molecule, PARP (Fig. 4G; Supplementary Fig. S2).

Mechanism of Mitochondrial Apoptotic Pathway Activation by ER Stress

Staurosporine-mediated mitochondrial damage induced the cleavage of caspase-9 and the subsequent activation of caspase-3 and PARP. This cascade of events is well recognized as the intrinsic apoptotic pathway in a wide range of cell types (Fig. 5A). We next examined CHOP, which is activated during chronic UPR by PERK and its downstream signal, and represents a transcription factor that regulates proapoptotic genes. Western blotting showed that treatment with thapsigargin, tunicamycin, and MG132 upregulated CHOP together with chaperone protein, but these responses were not observed following staurosporine treatment (Fig. 5B). Thapsigargin upregulated CHOP and activated caspase-9, whereas knockdown of CHOP by siRNA attenuated the downregulation of caspase-9 cleavage (Fig. 5C). The upregulation of GRP78 induced by thapsigargin was not altered by knockdown of CHOP.

Correspondingly, JC-1 staining showed that reduction of mitochondrial membrane potential by thapsigargin was prevented by siRNA-mediated knockdown of CHOP (Fig. 5D). These data suggest that activation of CHOP by the UPR triggers the intrinsic pathway associated with the alterations in both mitochondrial morphology and function. Based on these data, we proposed that excessive production of ECM proteins, including type I collagen and fibronectin, causes aggregation of unfolded or misfolded proteins and subsequent induction of the UPR. This UPR activation, in turn, triggers a cascade of molecular events that lead to apoptotic cell death by activation of the intrinsic apoptotic pathway (Fig. 5E).

Discussion

Prolonged UPR activation, caused by unmitigated ER stress and impaired homeostasis, induces cell death.[9,10,12] Following an impairment of homeostasis, the UPR serves as an apoptosis executor. This phenomenon has been accepted as indicating that the function of UPR-mediated apoptosis is to protect the organism from damaged cells that cannot ascertain the normal signaling components.[9] The "life or death" decision by the UPR serves as a universal underlying mechanism in the pathogenesis of various diseases, including neurodegenerative diseases, inflammation, metabolic disorders, liver dysfunction, and cancer.[9,10,13] For instance, accumulating evidence now supports a linkage of protein misfolding and inclusion body formation with neurodegenerative diseases, such as Alzheimer's disease, Parkinson's disease, and Huntington's disease.[23–26] In the field of eye disease, misfolded proteins and subsequent UPR signaling are related to pathogenesis in certain types of retinitis pigmentosa and Stargart-like macular degeneration.[27]

In the current study, we showed that excessive ECM proteins form aggregations of unfolded proteins in the corneal endothelium of FECD patients. The phenotypic clinical

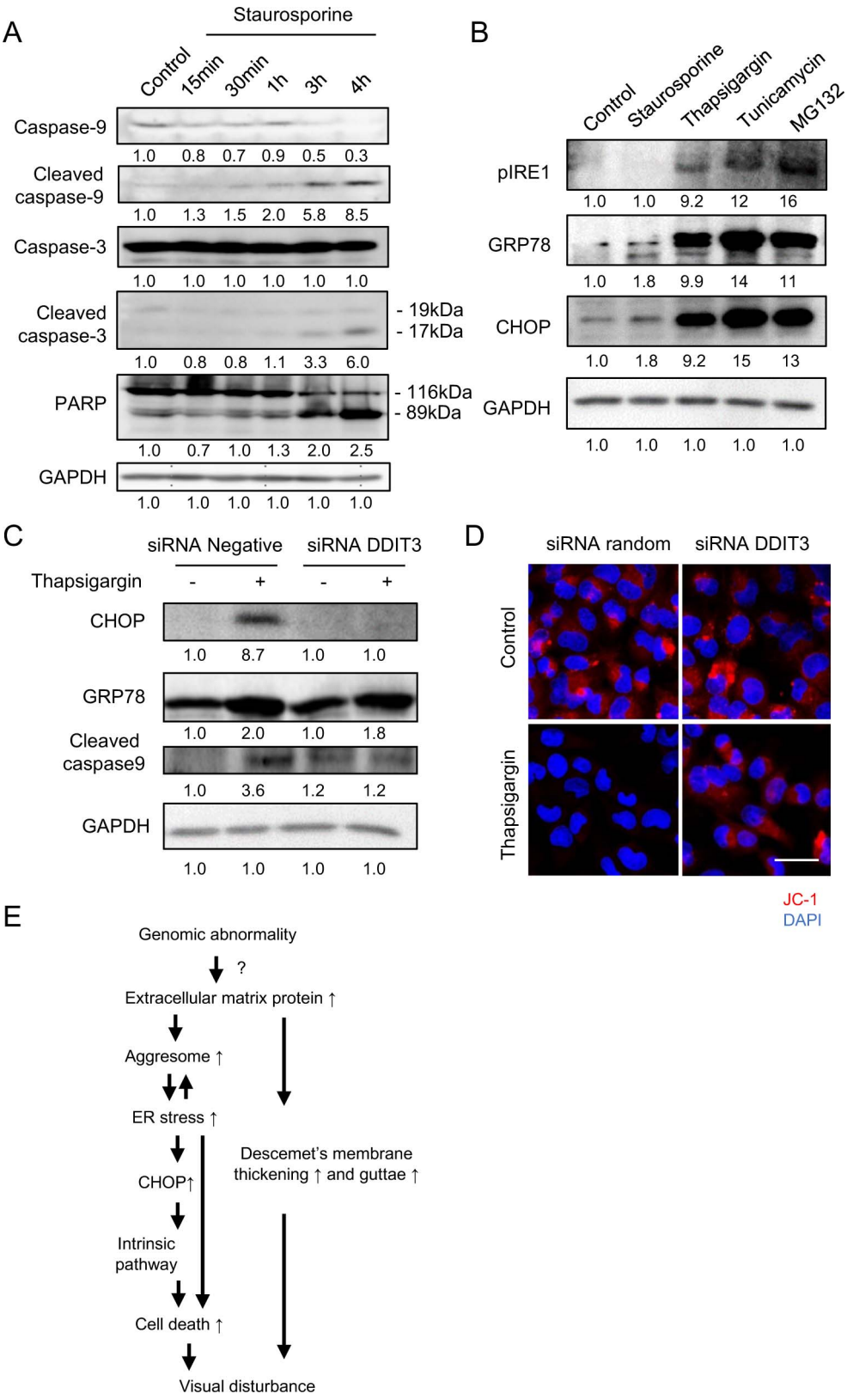

Figure 5. Involvement of CHOP as a "communicator" between the ER and the mitochondria during apoptosis. (**A**) iHCEC were cultured and then stimulated with staurosporine. Western blotting showed that staurosporine-mediated mitochondrial damage induces cleavage of caspase-9, caspase-3, and PARP. The relative density of immunoblot bands in duplicate experiments was determined using ImageJ software. Relative fold differences were compared with the values of the control. (**B**) iHCEC were treated with staurosporine, thapsigargin, tunicamycin, and MG132. Western blotting showed that thapsigargin, tunicamycin, and MG132 upregulated CHOP and GRP78. However, staurosporine did not upregulate CHOP. The relative density of immunoblot bands in duplicate experiments was determined using ImageJ software. Relative fold differences were compared with the values of the control. (**C**) iHCEC were incubated with RNAi duplex (DDIT3) and CHOP was knocked down. Thapsigargin increased CHOP and

activated caspase-9 in random siRNA controls. However, knockdown of CHOP by siRNA attenuated the caspase-9 cleavage. Induction of GRP78 by thapsigargin was not altered by knockdown of CHOP. The relative density of immunoblot bands in duplicate experiments was determined using ImageJ software. Relative fold differences were compared with the values of control. (**D**) Stimulation of iHCEC with knockdown of CHOP by siRNA and control iHCEC by thapsigargin. JC-1 staining shows depolarization of the mitochondrial membrane by thapsigargin in the control, but this was counteracted by knockdown of CHOP by siRNA. *Scale bar*: 50 μm. (**E**) Schematic image of our hypothetic pathophysiology was shown. Hyperproduction of ECM proteins and proteoglycans cause aggregation of unfolded or misfolded protein, and then induce unfolded protein response. A sustained unfolded protein response may at least partially activate the mitochondrial pathway through CHOP and induce apoptosis, as well as cause apoptosis through a mitochondria-independent pathway.

features of FECD are corneal guttae that are excrescences of the Descemet's membrane. Earlier studies demonstrated that certain types of ECM proteins and proteoglycans accumulate and form the guttae and thickening of Descemet's membrane.[19,20,28] Consistent with the general understanding that increased secretory protein production can trigger the formation of unfolded proteins in the ER lumen,[9] these accumulated proteins form aggregations of unfolded proteins in the FECD corneal endothelium. Although speculative, this idea may explain the clinical features, in which accumulation of ECM proteins is accompanied by a gradual loss of the corneal endothelium. We recently reported that high expression of genes inducing the epithelial mesenchymal transition (EMT) was involved in an excessive production of ECM proteins through the transforming growth factor (TGF)-β signaling pathway.[16] In addition, we postulated that the regulation of EMT-related genes, by counteracting this TGF-β signaling, may suppress the excessive production of ECM proteins.[16] Further study is required to determine whether suppression of excessive ECM production by inhibition of TGF-β signaling also represses the UPR; however, modulation of excessive protein production might be worth investigating as a therapeutic target for FECD treatment.

Three principal signal transducers (ATF6, PERK, and IRE1) that sense the protein folding conditions in the ER lumen have been identified.[9,29] Expression of these UPR transducers varies depending on tissues and cell types, but we have shown that all three signal transducers are conserved in the corneal endothelium and are activated by ER stress. ATF6 is expressed in the ER lumen, and unfolded protein accumulation causes delivery of ATF6 to the Golgi apparatus, whereas cleavage of the N-terminal cytosolic fragment results in activation of UPR target genes.[30] Consistently, we demonstrated that GRP78, a target gene of ATF6,[30] is highly expressed in FECD samples. When IRE1 senses unfolded protein, it cleaves the mRNA encoding X-box binding protein 1 (XBP1) and induces the spliced active form of XBP1. XBP1 regulates transcription of chaperones and ER-associated degradation components.[31]

PERK phosphorylates itself on sensing ER stress, and reduces mRNA translation by inactivating eIF2. Inactivation of eIF2 then increases ATF4, which in turn drives the expression of its target genes. One of the important target genes is CHOP, a transcription factor that regulates genes involved in apoptosis. PERK acts as protector of unfolded proteins, but it also contributes to cell death when the UPR reaches a critical level.[10,32] In the current study, we showed that a cell model derived from patients with FECD expressed higher levels of CHOP and this was associated with unfolded protein accumulation. In addition, knockdown of CHOP by siRNA suppressed the induction of the intrinsic apoptotic pathway by ER stress, indicating that CHOP activation due to ER stress triggers cell loss.

ER stress is transmitted to mitochondria by stress responsive signaling pathways or by altered transfer of metabolites such as Ca^{2+}.[10,33] Stress signaling from the ER to mitochondria results in prosurvival or proapoptotic responses in mitochondrial function, depending on the strength of the stress. Chronic exposure to ER stress reduces mitochondrial respiration and decreases cellular ATP levels, resulting in increases in Ca^{2+} in the mitochondria.[34] This subsequently induces mitochondrial fragmentation and elevation of mitochondrial permeability, which then initiates the intrinsic apoptotic signaling pathway.[10,35,36] We showed that the ultrastructure of mitochondria is altered in the corneal endothelium of patients with FECD. We also demonstrated that ER stress is transmitted to these mitochondria and initiates intrinsic apoptosis, whereas staurosporine-mediated apoptosis associated with dysfunction of mitochondria does not induce ER stress.

We postulate that the pathophysiology induced by apoptosis in response to chronic ER stress plays a central role in the progressive cell loss associated with FECD. In various cell types, ER stress affects mitochondrial DNA biogenesis and increases mitochondrially derived reactive oxygen species.[35–37] An involvement of mitochondrial dysfunction has consistently been suggested to play a role in FECD. For example, mitochondrial DNA damage repair was disturbed, mitochondrial DNA was degraded,[38] and antioxidant and oxidative stress–related gene expression were altered in FECD.[39]

In conclusion, the accumulation of excessive amounts of ECM proteins in FECD causes the accumulation of unfolded protein, and this might be associated with cell death through the intrinsic apoptotic signaling pathway. Further studies are needed, but inhibiting the intrinsic apoptotic pathway that arises as a UPR response might be a therapeutic target for FECD treatment.

Acknowledgments

Supported by the Program for the Strategic Research Foundation at Private Universities from MEXT (NK, NO).

Disclosure: **N. Okumura**, None; **M. Kitahara**, None; **H. Okuda**, None; **K. Hashimoto**, None; **E. Ueda**, None; **M. Nakahara**, None; **S. Kinoshita**, None; **R.D. Young**, None; **A.J. Quantock**, None; **T. Tourtas**, None; **U. Schlötzer-Schrehardt**, None; **F. Kruse**, None; **N. Koizumi**, None

References

1. Lorenzetti DW, Uotila MH, Parikh N, Kaufman HE. Central cornea guttata. Incidence in the general population. *Am J Ophthalmol*. 1967;64:1155–1158.
2. Eye Bank Association of America. Eye Banking Statistical Report. Washington, DC; 2014.
3. Borderie VM, Baudrimont M, Vallee A, Ereau TL, Gray F, Laroche L. Corneal endothelial cell apoptosis in patients with Fuchs' dystrophy. *Invest Ophthalmol Vis Sci*. 2000;41:2501–2505.
4. Li QJ, Ashraf MF, Shen DF, et al. The role of apoptosis in the pathogenesis of Fuchs endothelial dystrophy of the cornea. *Arch Ophthalmol*. 2001;119:1597–1604.
5. Szentmary N, Szende B, Suveges I. Epithelial cell, keratocyte, and endothelial cell apoptosis in Fuchs' dystrophy and in pseudophakic bullous keratopathy. *Eur J Ophthalmol*. 2005;15:17–22.

6. Engler C, Kelliher C, Spitze AR, Speck CL, Eberhart CG, Jun AS. Unfolded protein response in Fuchs endothelial corneal dystrophy: a unifying pathogenic pathway? *Am J Ophthalmol*. 2010;149:194–202.e2.
7. Jun AS, Meng H, Ramanan N, et al. An alpha 2 collagen VIII transgenic knock-in mouse model of Fuchs endothelial corneal dystrophy shows early endothelial cell unfolded protein response and apoptosis. *Hum Mol Genet*. 2012;21:384–393.
8. Ellgaard L, Helenius A. Quality control in the endoplasmic reticulum. *Nat Rev Mol Cell Biol*. 2003;4:181–191.
9. Walter P, Ron D. The unfolded protein response: from stress pathway to homeostatic regulation. *Science*. 2011;334:1081–1086.
10. Rainbolt TK, Saunders JM, Wiseman RL. Stress-responsive regulation of mitochondria through the ER unfolded protein response. *Trends Endocrinol Metab*. 2014;25:528–537.
11. Smith MH, Ploegh HL, Weissman JS. Road to ruin: targeting proteins for degradation in the endoplasmic reticulum. *Science*. 2011;334:1086–1090.
12. Tabas I, Ron D. Integrating the mechanisms of apoptosis induced by endoplasmic reticulum stress. *Nat Cell Biol*. 2011;13:184–190.
13. Jiang D, Niwa M, Koong AC. Targeting the IRE1alpha-XBP1 branch of the unfolded protein response in human diseases. *Semin Cancer Biol*. 2015;33:48–56.
14. Rozpedek W, Markiewicz L, Diehl JA, Pytel D, Majsterek I. Unfolded protein response and PERK kinase as a new therapeutic target in the pathogenesis of Alzheimer's disease. *Curr Med Chem*. 2015;22:3169–3184.
15. Hekmatimoghaddam S, Zare-Khormizi MR, Pourrajab F. Underlying mechanisms and chemical/biochemical therapeutic approaches to ameliorate protein misfolding neurodegenerative diseases [published online ahead of print February 22, 2016]. *Biofactors*. doi:10.1002/biof.1264.
16. Okumura N, Minamiyama R, Ho LT, et al. Involvement of ZEB1 and Snail1 in excessive production of extracellular matrix in Fuchs endothelial corneal dystrophy. *Lab Invest*. 2015;95:1291–1304.
17. Okumura N, Sakamoto Y, Fujii K, et al. Rho kinase inhibitor enables cell-based therapy for corneal endothelial dysfunction. *Sci Rep*. 2016;6:26113.
18. Mayer MP, Bukau B. Hsp70 chaperones: cellular functions and molecular mechanism. *Cell Mol Life Sci*. 2005;62:670–684.
19. Bourne WM, Johnson DH, Campbell RJ. The ultrastructure of Descemet's membrane. III. Fuchs' dystrophy. *Arch Ophthalmol*. 1982;100:1952–1955.
20. Weller JM, Zenkel M, Schlotzer-Schrehardt U, Bachmann BO, Tourtas T, Kruse FE. Extracellular matrix alterations in late-onset Fuchs' corneal dystrophy. *Invest Ophthalmol Vis Sci*. 2014;55:3700–3708.
21. Wu J, Kaufman RJ. From acute ER stress to physiological roles of the Unfolded Protein Response. *Cell Death Differ*. 2006;13:374–384.
22. Lytton J, Westlin M, Hanley MR. Thapsigargin inhibits the sarcoplasmic or endoplasmic reticulum Ca-ATPase family of calcium pumps. *J Biol Chem*. 1991;266:17067–17071.
23. Halliday M, Mallucci GR. Targeting the unfolded protein response in neurodegeneration: a new approach to therapy. *Neuropharmacology*. 2014;76:169–174.
24. Halliday M, Mallucci GR. Review: modulating the unfolded protein response to prevent neurodegeneration and enhance memory. *Neuropathol Appl Neurobiol*. 2015;41:414–427.
25. Huang HC, Tang D, Lu SY, Jiang ZF. Endoplasmic reticulum stress as a novel neuronal mediator in Alzheimer's disease. *Neurol Res*. 2015;37:366–374.
26. Scheper W, Hoozemans JJ. The unfolded protein response in neurodegenerative diseases: a neuropathological perspective. *Acta Neuropathol*. 2015;130:315–331.
27. Lin JH, Lavail MM. Misfolded proteins and retinal dystrophies. *Adv Exp Med Biol*. 2010;664:115–121.
28. Gottsch JD, Zhang C, Sundin OH, Bell WR, Stark WJ, Green WR. Fuchs corneal dystrophy: aberrant collagen distribution in an L450W mutant of the COL8A2 gene. *Invest Ophthalmol Vis Sci*. 2005;46:4504–4511.
29. Winnay JN, Kahn CR. PI 3-kinase regulatory subunits as regulators of the unfolded protein response. *Methods Enzymol*. 2011;490:147–158.
30. Haze K, Yoshida H, Yanagi H, Yura T, Mori K. Mammalian transcription factor ATF6 is synthesized as a transmembrane protein and activated by proteolysis in response to endoplasmic reticulum stress. *Mol Biol Cell*. 1999;10:3787–3799.
31. Reimold AM, Iwakoshi NN, Manis J, et al. Plasma cell differentiation requires the transcription factor XBP-1. *Nature*. 2001;412:300–307.
32. Tsaytler P, Harding HP, Ron D, Bertolotti A. Selective inhibition of a regulatory subunit of protein phosphatase 1 restores proteostasis. *Science*. 2011;332:91–94.
33. Bravo R, Vicencio JM, Parra V, et al. Increased ER-mitochondrial coupling promotes mitochondrial respiration and bioenergetics during early phases of ER stress. *J Cell Sci*. 2011;124:2143–2152.
34. Rizzuto R, De Stefani D, Raffaello A, Mammucari C. Mitochondria as sensors and regulators of calcium signalling. *Nat Rev Mol Cell Biol*. 2012;13:566–578.
35. Harding HP, Zhang Y, Zeng H, et al. An integrated stress response regulates amino acid metabolism and resistance to oxidative stress. *Mol Cell*. 2003;11:619–633.
36. Zheng M, Kim SK, Joe Y, et al. Sensing endoplasmic reticulum stress by protein kinase RNA-like endoplasmic reticulum kinase promotes adaptive mitochondrial DNA biogenesis and cell survival via heme oxygenase-1/carbon monoxide activity. *FASEB J*. 2012;26:2558–2568.
37. Cullinan SB, Diehl JA. PERK-dependent activation of Nrf2 contributes to redox homeostasis and cell survival following endoplasmic reticulum stress. *J Biol Chem*. 2004;279:20108–20117.
38. Czarny P, Seda A, Wielgorski M, et al. Mutagenesis of mitochondrial DNA in Fuchs endothelial corneal dystrophy. *Mutat Res*. 2014;760:42–47.
39. Jurkunas UV, Bitar MS, Funaki T, Azizi B. Evidence of oxidative stress in the pathogenesis of Fuchs endothelial corneal dystrophy. *Am J Pathol*. 2010;177:2278–2289.

Investigative Ophthalmology & Visual Science